Ocean Sci. Discuss., https://doi.org/10.5194/os-2018-75
Manuscript under review for journal Ocean Sci.
Discussion started: 23 July 2018

Ocean Science Discussions
Open Access

Measuring rates of present-day relative sea-level rise in low-elevation coastal zones: A critical evaluation

Molly E. Keogh[1] and Torbjörn E. Törnqvist

Department of Earth and Environmental Sciences, Tulane University, 6823 St. Charles Avenue, New Orleans, Louisiana 70118-5698, USA

[1]Corresponding author: mkeogh@tulane.edu

Ocean Sci. Discuss., https://doi.org/10.5194/os-2018-75
Manuscript under review for journal Ocean Sci.
Discussion started: 23 July 2018

1. ABSTRACT

Although tide gauges are the primary source of data used to calculate multi-decadal to century-scale rates of relative sea-level change, we question the reliability of tide-gauge data in rapidly subsiding low-elevation coastal zones (LECZs). Tide gauges measure relative sea-level rise (RSLR) with respect to the base of associated benchmarks. Focusing on coastal Louisiana, the largest LECZ in the United States, we find that these benchmarks (n = 35) are anchored an average of 21.5 m below the land surface. Because at least 60% of subsidence occurs in the top 5-10 m of the sediment column in this area, tide gauges in coastal Louisiana do not capture the primary contributor to RSLR. Similarly, GPS stations (n = 10) are anchored an average of >14.3 m below the land surface and therefore also do not capture shallow subsidence. As a result, tide gauges and GPS stations in coastal Louisiana, and likely in LECZs worldwide, systematically underestimate rates of RSLR as experienced at the land surface. We present an alternative approach that explicitly measures RSLR in LECZs with respect to the land surface and eliminates the need for tide-gauge data. Shallow subsidence is measured by rod surface-elevation table–marker horizons (RSET-MHs) and added to measurements of deep subsidence from GPS data, plus sea-level rise from satellite altimetry. We show that for a LECZ the size of coastal Louisiana (25,000-30,000 km^2), about 40 RSET-MH instruments suffice to collect useful data. Rates of RSLR obtained from this approach are substantially higher than rates as inferred from tide-gauge data. We therefore conclude that LECZs may be at higher risk of flooding, and within a shorter time horizon, than previously assumed.

2. INTRODUCTION

In the current era of accelerated sea-level rise, accurate measurements of relative sea-level change are critical to predict the conditions that coastal areas will face in coming decades and beyond. Such measurements traditionally come from tide gauges, which provide the longest available instrumental records of relative sea-level rise (RSLR). Some of the oldest tide gauges have records spanning 150-200+ years (e.g. Brest, France; Świnoujście, Poland; New York, USA). Tide-gauge data have played a central role in calculations of global sea-level rise (e.g. Gornitz et al., 1982) and they continue to do so today (e.g. Church and White, 2011; Church et al., 2013; Hay et al., 2015; Watson et al., 2015).

Tide-gauge data are also heavily relied upon to evaluate the vulnerability of low-elevation coastal zones (LECZs) (e.g. Syvitski et al., 2009; Nicholls and Cazenave, 2010; Kopp et al., 2014; Pfeffer and Allemand, 2016). LECZs include large deltas and coastal plains that often have accumulated thick packages (tens of meters or more) of highly compressible Holocene strata and are the home to some of the world's largest population centers (e.g. Tokyo, Shanghai, Bangkok, Manila) that are increasingly at risk due to RSLR. At the regional level, tide-gauge data have been used to study a variety of spatially variable processes. For example, in coastal Louisiana, the largest LECZ in the United States, tide-gauge data have been used to measure land subsidence (Swanson and Thurlow, 1973), the acceleration of RSLR (Nummedal,

Ocean Sci. Discuss., https://doi.org/10.5194/os-2018-75
Manuscript under review for journal Ocean Sci.
Discussion started: 23 July 2018

1983), multi-decadal rates of subsidence and RSLR (Penland and Ramsey, 1990), and the impact of fluid extraction on RSLR (Kolker et al., 2011).

The Permanent Service for Mean Sea Level (PSMSL) maintains records for nearly 2000 tide gauges globally, including five located in coastal Louisiana. In many parts of the world, however, tide gauges with long, continuous records are few and far between. As a result, many studies of RSLR rely on tide-gauge records that are too short (longer than 50 years is preferable but at least 30 years is necessary to filter out natural variability; Pugh, 1987; Douglas, 1991; Shennan and Woodworth, 1992), are from inappropriate locations (e.g. outside of the area being studied), or both. For example, of the 32 tide gauges used by Syvitski et al. (2009), 21 were located outside the delta of interest, 11 had records of <30 years, and 8 had both shortcomings. Furthermore, subsidence rates are highly spatially variable, often increasing or decreasing 2- to 4-fold within short distances (a few km or less) as a result of subsurface fluid withdrawal and differential compaction, among other factors (e.g. Teatini et al., 2005; Törnqvist et al., 2008; Minderhoud et al., 2017; Koster et al., 2018; also see the review by Higgins, 2016). As a result, tide gauges provide limited information on subsidence rates beyond the instrument's immediate surroundings. Even if a tide gauge has a sufficiently long record and is appropriately located, it is critical to determine what processes the tide gauge is measuring, and what it is not measuring. In LECZs, this is commonly not straightforward.

Tide gauges measure RSLR with respect to a nearby set of benchmarks. Leveling campaigns are conducted regularly (for example, at least once every six months for NOAA tide gauges) to account for any changes in the elevation of the tide gauge with respect to these reference points. Figure 1 shows a schematic of tide gauges and associated benchmarks in three contrasting environments. Along rocky coastlines, benchmarks are typically anchored directly onto bedrock that is exposed at the surface (Fig. 1a). A tide gauge in such a setting therefore measures RSLR with respect to the land surface. In contrast, benchmarks in LECZs are typically anchored at depth. In thin LECZs, which are defined herein as those with unconsolidated sediment packages <20 m thick, benchmark foundations typically penetrate the surficial layer of unconsolidated (usually Holocene) sediment and are anchored in the underlying consolidated (usually Pleistocene) strata (Fig. 1b). In thick LECZs, defined as possessing unconsolidated sediment packages that are >20 m thick, benchmark foundations are generally not sufficiently deep to reach the consolidated strata and are anchored within the unconsolidated sediment (Fig. 1c).

Regardless of the environment, all tide gauges measure changes in water surface elevation with respect to the foundation depth of their associated benchmarks. As a result, tide gauges with benchmarks anchored at depth do not account for processes occurring in the shallow subsurface, above the benchmark foundation. For the purposes of this study, we define the subsidence that occurs above a benchmark's foundation as "shallow subsidence". Subsidence below a benchmark's foundation is termed "deep subsidence". In coastal Louisiana, at least 60% of subsidence occurs in the shallowest 5-10 meters (Cahoon et al., 1995; Jankowski et al., 2017). Tide gauges with benchmarks anchored at depth do not record this key component of RSLR.

Ocean Sci. Discuss., https://doi.org/10.5194/os-2018-75
Manuscript under review for journal Ocean Sci.
Discussion started: 23 July 2018

In order to better understand the contribution of vertical ground motion to RSLR, tide-gauge data are often used in conjunction with global positioning system (GPS) data (e.g. Mazzotti et al., 2009; Wöppelmann et al., 2009; Wöppelmann and Marcos, 2016). In LECZs, GPS stations are typically mounted on existing buildings or attached to rods that are driven to refusal (i.e. the depth at which friction prevents deeper penetration) and record the deep subsidence that occurs beneath their foundations. Similar to tide gauges, GPS stations are nearly always anchored at depth and thus face many of the same concerns: they do not record shallow subsidence that occurs in the strata above the depth of their foundations.

Accurate measurements of RSLR are vital to predict the sustainability of world deltas and for communities in LECZs to adapt to their changing coastlines. In this study, we investigate the nature of tide gauge benchmarks and GPS station foundations in coastal Louisiana and assess the implications for measurements of RSLR and subsidence in LECZs worldwide. Re-analysis of time series from tide gauges and GPS stations is not the purpose of our study. Instead, we present an alternative approach to measuring RSLR in LECZs where shallow subsidence is determined using the rod surface-elevation table–marker horizon method (RSET-MH; Webb et al., 2013; Cahoon, 2015) and deep subsidence is determined using GPS data. Using the Mississippi Delta (a thick LECZ) and the Chenier Plain (a thin LECZ) in coastal Louisiana as the primary study areas, we determine foundation depths and the type of strata in which the foundations are anchored. This allows us to determine which subsidence processes are measured by tide gauges and GPS stations and to evaluate their usefulness as recorders of RSLR. We then place our findings in the context of LECZs worldwide. Our results suggest that tide gauges (and existing analyses of tide-gauge data) in these environments may underestimate rates of RSLR as observed at the land surface, and as a result, many LECZs may be at higher risk of submergence than previously recognized.

3. DATA AND METHODS

Relative sea level and subsidence data are abundant in the Mississippi Delta and Chenier Plain, making coastal Louisiana an excellent target to assess methods of measuring RSLR. Records for at least 131 operational or previously operational tide gauges in this region are maintained by the National Oceanic and Atmospheric Administration (NOAA; https://tidesandcurrents.noaa.gov), the U.S. Army Corps of Engineers (USACE; http://www.rivergages.com and USACE 2015), and the U.S. Geological Survey (USGS; http://nwis.waterdata.usgs.gov). Although 37 of these tide gauges have records spanning more than 30 years, many of their records are incomplete and have large data gaps. Many other tide gauges in coastal Louisiana have extremely short records; nearly half have time series <10 years, and a quarter are <2 years long (see Table S1 for information on all 131 tide gauges).

By means of exhaustive record combing of NOAA, USACE, and USGS archives, benchmark foundation depths were determined for tide gauges located in the Holocene landscape of the Mississippi Delta and Chenier Plain. Foundation depths were then compared to the local elevation of the Pleistocene surface (with respect to the North American Vertical Datum of 1988, NAVD 88). Because the land surface elevations at the tide gauge locations are close to sea level, the elevation of the Pleistocene surface is essentially equivalent to its depth beneath the land surface.

A similar approach was taken to determine foundation depths of GPS stations. GPS station information was compiled from Dokka et al. (2006) and Karegar et al. (2015). Of the 45 GPS stations used for analysis by one or both studies, 17 are located in the Holocene landscape of coastal Louisiana. GPS station foundation depths were compared to the local depth of the Pleistocene surface, similar to what was done for the tide gauges.

4. RESULTS

The 131 tide gauges in coastal Louisiana were examined for benchmark information (Table 1, Fig. 2). Benchmark foundation depths are available for only 35 tide gauges (Table 1), including 31 maintained by NOAA and 4 maintained by USACE (see Table S1 for information on all 131 tide gauges). Each of the NOAA tide gauges is associated with 3 to 11 benchmarks (mean = 6 benchmarks), 77% of which have known foundation depths. The total number of associated benchmarks is unknown for the USACE tide gauges. The remaining 96 tide gauges (73% of the total) have no available benchmark foundation information.

For tide gauges with available benchmark information, benchmark foundation depths range from 0.9 to 35.1 m, with a mean of 21.5 ± 7.4 m and a median of 23.2 m. When a tide gauge is associated with multiple benchmarks, the benchmark with the deepest known foundation was used for this analysis. Figure 3 shows the location of tide gauges in coastal Louisiana (circles) and the foundation depth of their associated benchmarks relative to the local depth to the Pleistocene surface. The depth to the Pleistocene surface from the land surface at tide gauge locations ranges from 5 to 142 m, with a mean of 47 ± 34 m and a median of 44 m (Fig. 4). Thus, benchmark foundations are anchored an average of 25.5 m above the Pleistocene surface. Only 11 of the 35 tide gauges (31%) have benchmarks anchored in Pleistocene strata; the remaining 24 tide gauges (69%) have benchmarks anchored in Holocene strata.

Of the 17 GPS stations in coastal Louisiana, 10 (59%) have known foundation depths (Table 2, Fig. 3). Information for all 17 GPS stations in coastal Louisiana is available in Table S2. Foundation depths of the 10 GPS stations range from 1 to 36.5 m, with a mean of >14.3 ± 11.9 m and a median of 14.9 m (Table 2). Note that for two GPS stations only minimum foundation depths are available; these minimum values are used in the analysis in order to produce conservative results. At GPS station locations, the depth to the Pleistocene surface ranges from 10 to 78 m, with a mean of 38.5 ± 20.4 m and a median of 34.5 m (Fig. 4). Thus, GPS station foundations are anchored an average of 24.2 m above the Pleistocene surface. Only one of the 10 GPS stations (10%) is anchored in Pleistocene strata, whereas the remaining 9 GPS stations (90%) are anchored in Holocene strata. Figure 3 shows the location of GPS stations in coastal Louisiana (squares) and their foundation depth relative to the local depth to the Pleistocene surface.

5. DISCUSSION

5.1. Implications for the interpretation of tide gauge and GPS records

In coastal Louisiana, foundation information for tide gauge benchmarks and GPS stations is often not available, essentially precluding the interpretation of resulting time series in terms of rates of RSLR. However, because all tide gauge benchmarks with available foundation information are anchored at depth rather than at ground level, and most (91%) are anchored well below the land surface (>10 m), their interpretation is far from straightforward. Tide gauges with benchmarks anchored at depth measure deep subsidence plus the eustatic component of RSLR as well as other oceanographic effects, but do not capture shallow subsidence, often a dominant element of total subsidence in this region. Similarly, all GPS stations are anchored at depth (60% are anchored >10 m deep) and also do not record shallow subsidence. Thus, tide gauges and GPS stations in coastal Louisiana systematically underestimate the rates of local RSLR and subsidence, respectively.

If a tide gauge benchmark is anchored in Pleistocene deposits, deep subsidence consists solely of subsidence within the Pleistocene and underlying strata (Fig. 1b). This scenario is common in LECZs with a relatively thin Holocene sediment package, such as the Chenier Plain. In the Chenier Plain, the Pleistocene surface subsides at a rate of ~1 mm yr^{-1}, yet the wetland surface is subsiding notably faster, at a rate of 7.5 mm yr^{-1} on average (Jankowski et al., 2017). The remaining 6.5 mm yr^{-1} of shallow subsidence occurs above the depth of local benchmark foundations and is typically not captured by tide gauges in this region.

In the case of a benchmark that is anchored in Holocene strata, deep subsidence also includes subsidence of the underlying Holocene sediments. This scenario (Fig. 1c) is common in LECZs with thick sediment packages such as the Mississippi Delta, and further complicates the interpretation of tide-gauge data. Compaction of deeper Holocene strata may result in an increase in the measured rate of RSLR when compared to tide gauges with benchmarks anchored in Pleistocene strata. However, tide gauges with benchmarks anchored in Holocene strata still record rates of RSLR that are considerably lower than what is seen at the land surface (13 ± 9 mm yr^{-1}; Jankowski et al., 2017). For example, Kolker et al. (2011) and Karegar et al. (2015) calculated modern RSLR rates from tide-gauge data in the Mississippi Delta of ~3 mm yr^{-1} (after adding the long-term rate of RSLR measured at Pensacola, Florida) and at least ~7 mm yr^{-1}, respectively.

Around the world, many LECZs have sediment packages that exceed 20 m in thickness, and some are as thick as 100 m or more (Table 3). In such settings, tide gauges likely underestimate the local rate of RSLR. A lack of reliable RSLR data will be increasingly problematic in several large deltas that are home to major population centers (e.g. Ganges-Brahmaputra, Song Hong, Yangtze, Mekong, Nile) and are experiencing rapid subsidence (Alam, 1996; Mathers and Zalasiewicz, 1999; Shi et al., 2008; Erban et al., 2014; Gebremichael et al., 2018). In these areas and in LECZs globally, people and infrastructure may therefore be even more vulnerable to flooding than previously recognized (e.g. Syvitski et al., 2009; Tessler et al., 2015).

Ocean Sci. Discuss., https://doi.org/10.5194/os-2018-75
Manuscript under review for journal Ocean Sci.
Discussion started: 23 July 2018

Two studies that considered delta vulnerability on a global scale (Ericson et al., 2006; Tessler et al., 2015) are noteworthy because they did not depend on tide-gauge data. These studies determined RSLR by adding the historic eustatic sea-level rise to natural and anthropogenic subsidence data (Ericson et al., 2006) or by combining sea-level rise from satellite altimetry with subsidence estimates associated with fluid extraction (Tessler et al., 2015). While these approaches bypass the problems with tide gauges discussed above, they are also inherently limited by the need to characterize individual deltas by single metrics and/or by not considering all major subsidence processes (notably shallow compaction). In the next section, we build on the recent study by Jankowski et al. (2017) to offer an alternative approach to measure RSLR in LECZs.

5.2. An alternative method for measuring present-day rates of relative sea-level rise

In order to accurately measure present-day RSLR in LECZs, we propose an alternative approach that combines measurements of shallow subsidence from RSET-MHs with measurements of deep subsidence and the oceanic component of sea-level rise from GPS and satellite altimetry data, respectively (Fig. 5). This approach results in RSLR measurements expressed with respect to the land surface and eliminates the need for tide-gauge data. One limitation of this method is that RSET-MHs are only useful in wetland environments such as marshes (e.g. Day et al., 2011) and mangroves (e.g. Lovelock et al., 2015). However, space-based geodetic methods such as interferometric synthetic-aperture radar (InSAR) are effective at measuring subsidence rates (the sum of shallow and deep) in heavily human-modified delta environments (e.g. agricultural land), and thus can be complementary to RSET-MH datasets in this context. Ideally, RSET-MHs are installed with similar foundation depths as nearby GPS stations in order to confirm that the two instruments are neither duplicating nor missing subsidence intervals. In coastal Louisiana, however, 33% of GPS stations have no known foundation information, and this lack of information is likely a common phenomenon worldwide. Finally, the launch of the Surface Water and Ocean Topography (SWOT; https://swot.jpl.nasa.gov/home.htm) mission in 2021 is expected to significantly improve the quality of sea-surface records in the coastal zone and could therefore become an important element of the approach advocated here.

Currently, coastal Louisiana has nearly 350 RSET-MHs operated by the USGS as part of the Coastwide Reference Monitoring System (CRMS; https://lacoast.gov/crms2), which provide shallow subsidence data at high spatial resolution. Although data from a single RSET-MH are commonly too noisy to produce a reliable trend (Jankowski et al., 2017), partly because most RSET-MHs were installed within the last decade and thus have time series that are mostly <10 years long, such a high density of RSET-MHs is not necessary to produce adequate estimates of shallow subsidence rates for a wider region. Using a Monte Carlo approach, we took random samples from subsets of the full RSET-MH dataset for coastal Louisiana (n = 274) to determine the smallest sample size that would still produce reasonable outcomes with an acceptable error. While determining the acceptable error is inherently somewhat arbitrary, the results show that in coastal Louisiana a minimum of 40 RSET-MHs would be needed in order to produce a mean shallow subsidence rate with a sufficiently narrow 95% confidence interval (4.54–9.18 mm yr^{-1}; Figs. 6 and S1). In terms of density and given the size of coastal Louisiana (25,000-30,000 km^2), we estimate that two RSET-MHs per 1000 km^2 would suffice. Although this density is slightly higher than strictly needed in coastal Louisiana, it is conceivable that higher densities may be necessary in smaller LECZs.

In addition, averaging data from at least 40 RSET-MHs will encompass the high spatial variability commonly seen in shallow subsidence. In coastal Louisiana, spatial correlation in subsidence rates is largely limited to distances <5 km, and no correlation exists beyond 25 km (Nienhuis et al., 2017). As a result, the relevance of a single measurement of shallow subsidence is limited to the area immediately around the instrument. Today, tide gauges around the world are generally spaced tens if not hundreds of km apart (for example, the five PSMSL stations in Louisiana are spaced, on average, 95 km apart), and only a few are associated with RSET-MHs. Although this lack of data prevents comprehensive measurement of subsidence in most LECZs today, our ability to predict local rates of RSLR will improve as more RSET-MHs are added to a growing global network. We therefore echo Webb et al. (2013) who first proposed this type of global RSET-MH network, arguing that the instruments are low-cost and produce highly valuable measurements of shallow subsidence.

6. CONCLUSIONS

In the Mississippi Delta and Chenier Plain of coastal Louisiana, tide gauge benchmarks and GPS stations are anchored an average of 21.5 ± 7.4 m and >14.3 ± 11.9 m below the land surface, respectively. By comparison, the local depth to the Pleistocene surface averages 47 ± 34 m at tide gauge locations and 38.5 ± 20.4 m at GPS stations. Instruments located in the Chenier Plain, a thin LECZ with Holocene strata typically only 5-10 m thick, are generally anchored in consolidated Pleistocene strata. In the Mississippi Delta, a thick LECZ where the Holocene sediment package is an order of magnitude thicker, tide gauge benchmarks and GPS stations are typically anchored within unconsolidated Holocene strata and therefore produce time series that are very difficult to interpret. Instruments anchored at depth do not capture shallow subsidence, a major component of total subsidence. As a result, tide gauges and GPS stations in coastal Louisiana, and likely in LECZs worldwide, underestimate rates of RSLR and subsidence with respect to the land surface by a variable but unknown amount.

In order to accurately measure present-day RSLR in LECZs, we propose an alternative method which combines measurements of shallow subsidence from RSET-MHs with measurements of deep subsidence and the oceanic component of sea-level rise from GPS stations and satellite altimetry, respectively. This approach produces rates of RSLR that are explicitly tied to the land surface and eliminates the need for tide-gauge data. We find that for an area the size of coastal Louisiana, a minimum density of two RSET-MHs per 1000 km^2 is necessary in order to obtain robust shallow subsidence data. We support the call for a global network of RSET-MHs as first put forward by Webb et al. (2013). Data from such a global network will help refine existing plans for coastal adaptation that presently may be inadequate to deal with potentially higher-than-anticipated rates of RSLR.

7. ACKNOWLEDGEMENTS

This work was supported by the US National Science Foundation (EAR-1349311). We would like to thank Carl Swanson for writing the Python code to run the Monte Carlo analysis, and William Veatch for locating benchmark information for USACE tide gauges.

8. REFERENCES

Alam, M. 1996. Subsidence of the Ganges-Brahmaputra Delta of Bangladesh and associated drainage, sedimentation and salinity problems. In: J.D. Milliman and B.U. Haq, eds., Sea-Level Rise and Coastal Subsidence. Springer, Dordrecht, the Netherlands, 169-192.

Amorosi, A., L. Bruno, D.M. Cleveland, A. Morelli, and W. Hong. 2017. Paleosols and associated channel-belt sand bodies from a continuously subsiding late Quaternary system (Po Basin, Italy): New insights into continental sequence stratigraphy. Geological Society of America Bulletin, 129, 449-463.

Cahoon, D.R. 2015. Estimating relative sea-level rise and submergence potential at a coastal wetland. Estuaries and Coasts, 38, 1077-1084.

Cahoon, D.R., D.J. Reed, and J.W. Day, Jr. 1995. Estimating shallow subsidence in microtidal salt marshes of the southeastern United States: Kaye and Barghoorn revisited. Marine Geology, 128, 1-9.

Church, J.A. and N.J. White. 2011. Sea-level rise from the late 19th to the early 21st century. Surveys in Geophysics, 32, 585-602.

Church, J.A., P.U. Clark, A. Cazenave, J.M. Gregory, S. Jevrejeva, A. Levermann, M.A. Merrifield, G.A. Milne, R.S. Nerem, P.D. Nunn, A.J. Payne, W.T. Pfeffer, D. Stammer, and A.S. Unnikrishnan. 2013. Sea Level Change. In: T.F. Stocker, D. Qin, G.-K. Plattner, M. Tignor, S.K. Allen, J. Boschung, A. Nauels, Y. Xia, V. Bex, and P.M. Midgley, eds., Climate Change 2013: The Physical Science Basis. Contribution of Working Group I to the Fifth Assessment Report of the Intergovernmental Panel on Climate Change. Cambridge University Press, New York, NY, USA, 1137-1216.

Clift, P.D., L. Giosan, A. Carter, E. Garzanti, V. Galy, A.R. Tabrez, M. Pringle, I.H. Campbell, C. France-Lanord, J. Blusztajn, C. Allen, A. Alizai, A. Lückge, M. Danish, and M.M. Rabbani. 2010. Monsoon control over erosion patterns in the Western Himalaya: possible feed-back into the tectonic evolution. Geological Society Special Publication, 342, 185-218.

Day, J., C. Ibáñez, F. Scarton, D. Pont, P. Hensel, J. Day, and R. Lane. 2011. Sustainability of Mediterranean deltaic and lagoon wetlands with sea-level rise: The importance of river input. Estuaries and Coasts, 34, 483-493.

Dokka, R.K., G.F. Sella, and T.H. Dixon. 2006. Tectonic control of subsidence and southward displacement of southeast Louisiana with respect to stable North America. Geophysical Research Letters, 33, L23308.

Ocean Sci. Discuss., https://doi.org/10.5194/os-2018-75
Manuscript under review for journal Ocean Sci.
Discussion started: 23 July 2018

Douglas, B.C. 1991. Global sea level rise. Journal of Geophysical Research, 96, 6981-6992.

Erban, L.E., S.M. Gorelick, and H.A. Zebker. 2014. Groundwater extraction, land subsidence, and sea-level rise in the Mekong Delta, Vietnam. Environmental Research Letters, 9, 084010.

Ericson, J.P., C.J. Vörösmarty, S.L. Dingman, L.G. Ward, and M. Meybeck. 2006. Effective sea-level rise and deltas: Causes of change and human dimension implications. Global and Planetary Change, 50, 63-82.

Funabiki, A., S. Haruyama, N. Van Quy, P. Van Hai, and D.H. Thai. 2007. Holocene delta plain development in the Song Hong (Red River) delta, Vietnam. Journal of Asian Earth Sciences, 30, 518-529.

Gebremichael, E., M. Sultan, R. Becker, M. El Bastawesy, O. Cherif, and M. Emil. 2018. Assessing land deformation and sea encroachment in the Nile Delta: A radar interferometric and inundation modeling approach. Journal of Geophysical Research: Solid Earth, 123, 3208-3224.

Goodbred, S.L. and S.A. Kuehl. 2000. The significance of large sediment supply, active tectonism, and eustasy on margin sequence development: Late Quaternary stratigraphy and evolution of the Ganges–Brahmaputra delta. Sedimentary Geology, 133, 227-248.

Gornitz, V., S. Lebedeff, and J. Hansen. 1982. Global sea level trend in the past century. Science, 215, 1611-1614.

Harris, P.T., E.K. Baker, A.R. Cole, and S.A. Short. A preliminary study of sedimentation in the tidally dominated Fly River Delta, Gulf of Papua. Continental Shelf Research, 13, 441-472.

Hay, C.C., E. Morrow, R.E. Kopp, and J.X. Mitrovica. 2015. Probabilistic reanalysis of twentieth-century sea-level rise. Nature, 517, 481-484.

Heinrich, P., R. Paulsell, R. Milner, J. Snead, and H. Peele. 2015. Investigation and GIS development of the buried Holocene-Pleistocene surface in the Louisiana coastal plain: Baton Rouge, LA, Louisiana Geological Survey-Louisiana State University for Coastal Protection and Restoration Authority of Louisiana, 140 p.

Higgins, S.A. 2016. Advances in delta-subsidence research using satellite methods. Hydrogeology Journal, 24, 587-600.

Hijma, M.P, K.M. Cohen, G. Hoffmann, A.J.F. van der Spek, and E. Stouthamer. 2009. From river valley to estuary: the evolution of the Rhine mouth in the early to middle Holocene (western Netherlands, Rhine-Meuse delta). Netherlands Journal of Geosciences, 88, 13-53.

Hori, K., S. Usami, and H. Ueda. 2011. Sediment facies and Holocene deposition rate of near-coastal fluvial systems: An example from the Nobi Plain, Japan. Journal of Asian Earth Sciences, 41, 195-203.

Jankowski, K.L., T.E. Törnqvist, and A.M. Fernandes. 2017. Vulnerability of Louisiana's coastal wetlands to present-day rates of relative sea-level rise. Nature Communications, 8, 14792.

Ocean Sci. Discuss., https://doi.org/10.5194/os-2018-75
Manuscript under review for journal Ocean Sci.
Discussion started: 23 July 2018

Ocean Science Discussions

Karegar, M.A., T.H. Dixon, and R. Malservisi. 2015. A three-dimensional surface velocity field for the Mississippi Delta: Implications for coastal restoration and flood potential. Geology, 43, 519-522.

Kolker, A.S., M.A. Allison, and S. Hameed. 2011. An evaluation of subsidence rates and sea-level variability in the northern Gulf of Mexico. Geophysical Research Letters, 38, L21404.

Kopp, R.E., R.M. Horton, C.M. Little, J.X. Mitrovica, M. Oppenheimer, D.J. Rasmussen, B.H. Strauss, and C. Tebaldi. 2014. Probabilistic 21st and 22nd century sea-level projections at a global network of tide-gauge sites. Earth's Future, 2, 383-406.

Koster, K., K.M. Cohen, J. Stafleu, and E. Stouthamer. 2018. Using ^{14}C-dated peat beds for reconstructing subsidence by compression in the Holland coastal plain of the Netherlands. Journal of Coastal Research, in press.

Larsen, C.E. 1975. The Mesopotamian Delta region: A reconsideration of Lees and Falcon. Journal of the American Oriental Society, 95, 43-57.

Li, C., Q. Chen, J. Zhang, S. Yang, and D. Fan. 2000. Stratigraphy and paleoenvironmental changes in the Yangtze Delta during the Late Quaternary. Journal of Asian Earth Sciences, 18, 453-469.

Lovelock, C.E., D.R. Cahoon, D.A. Friess, G.R. Guntenspergen, K.W. Krauss, R. Reef, K. Rogers, M.L. Saunders, F. Sidik, A. Swales, N. Saintilan, L.X. Thuyen, and T. Triet. 2015. The vulnerability of Indo-Pacific mangrove forests to sea-level rise. Nature, 526, 559-563.

Mathers, S. and J. Zalasiewicz. 1999. Holocene sedimentary architecture of the Red River Delta. Journal of Coastal Research, 15, 314-325.

Mazzotti, S., A. Lambert, M. Van der Kooij, and A. Mainville. 2009. Impact of anthropogenic subsidence on relative sea-level rise in the Fraser River delta. Geology, 37, 771-774.

Minderhoud, P.S.J., G. Erkens, V.H. Pham, V.T. Bui, L. Erban, H. Kooi, and E. Stouthamer. 2017. Impacts of 25 years of groundwater extraction on subsidence in the Mekong delta, Vietnam. Environmental Research Letters, 12, 064006.

Mojski, J.E. 1995. Geology and evolution of the Vistula Delta and Vistula Bar. Journal of Coastal Research, Special Issue, 22, 141-149.

Nicholls, R.J. and A. Cazenave. 2010. Sea-level rise and its impact on coastal zones. Science, 328, 1517-1520.

Nienhuis, J.H., T.E. Törnqvist, K.L. Jankowski, A.M. Fernandes, and M.E. Keogh. 2017. A new subsidence map for coastal Louisiana. GSA Today, 27 (9), 58-59.

Nummedal, D. 1983. Future sea level changes along the Louisiana coast. Shore and Beach, 51 (2), 10-15.

Penland, S. and K.E. Ramsey. 1990. Relative sea-level rise in Louisiana and the Gulf of Mexico: 1908-1988. Journal of Coastal Research, 6, 323-342.

Pfeffer, J. and P. Allemand. 2016. The key role of vertical land motions in coastal sea level variations: A global synthesis of multisatellite altimetry, tide gauge data and GPS measurements. Earth and Planetary Science Letters, 439, 39-47.

Pugh, D.T. 1987. Tides, Surges, and Mean Sea-Level. John Wiley, New York, 472 p.

Shennan, I. and P.L. Woodworth. 1992. A comparison of late Holocene and twentieth-century sea-level trends from the UK and North Sea region. Geophysical Journal International, 109, 96-105.

Shi, X., J. Wu, S. Ye, Y. Zhang, Y. Xue, Z. Wei, Q. Li, and J. Yu. 2008. Regional land subsidence simulation in Su-Xi-Chang area and Shanghai City, China. Engineering Geology, 100, 27-42.

Stanley, D.J. and A.G. Warne. 1993. Nile Delta: Recent geological evolution and human impact. Science, 260, 628-634.

Swanson, R.L. and C.I. Thurlow. 1973. Recent subsidence rates along the Texas and Louisiana coasts as determined from tide measurements. Journal of Geophysical Research, 78, 2665-2671.

Syvitski, J.P.M., A.J. Kettner, I. Overeem, E.W.H. Hutton, M.T. Hannon, G.R. Brakenridge, J. Day, C. Vörösmarty, Y. Saito, L. Giosan, and R.J. Nicholls. 2009. Sinking deltas due to human activities. Nature Geoscience, 2, 681-686.

Ta, T.K.O., V.L. Nguyen, M. Tateishi, I. Kobayashi, S. Tanabe, and Y. Saito. 2002. Holocene delta evolution and sediment discharge of the Mekong River, southern Vietnam. Quaternary Science Reviews, 21, 1807-1819.

Tanabe, S., Y. Saito, Y. Sato, Y. Suzuki, S. Sinsakul, S. Tiyapairach, and N. Chaimanee. 2003a. Stratigraphy and Holocene evolution of the mud-dominated Chao Phraya delta, Thailand. Quaternary Science Reviews, 22, 789-807.

Tanabe, S., T.K.O. Ta, V.L. Nguyen, M. Tateishi, I. Kobayashi, and Y. Saito. 2003b. Delta evolution model inferred from the Holocene Mekong delta, southern Vietnam. SEPM (Society for Sedimentary Geology) Special Publication, 76, 175-188.

Tanabe, S., T. Nakanishi, Y. Ishihara, and R. Nakashima. 2015. Millennial-scale stratigraphy of a tide-dominated incised valley during the last 14 kyr: Spatial and quantitative reconstruction in the Tokyo Lowland, central Japan. Sedimentology, 62, 1837-1872.

Teatini, P., L. Tosi, T. Strozzi, L. Carbognin, U. Wegmüller, and F. Rizzetto. 2005. Mapping regional land displacements in the Venice coastland by an integrated monitoring system. Remote Sensing of Environment, 98, 403-413.

Tessler, Z.D., C.J. Vörösmarty, M. Grossberg, I. Gladkova, H. Aizenman, J.P.M. Syvitski, and E. Foufoula-Georgiou. 2015. Profiling risk and sustainability in coastal deltas of the world. Science, 349, 638-643.

Törnqvist, T.E., D.J. Wallace, J.E.A. Storms, J. Wallinga, R.L. van Dam, M. Blaauw, M.S. Derksen, C.J.W. Klerks, C. Meijneken, and E.M.A. Snijders. 2008. Mississippi Delta subsidence primarily caused by compaction of Holocene strata. Nature Geoscience, 1, 173-176.

U.S. Army Corps of Engineers (USACE). 2015. 2015 updated atlas of U. S. Army Corps of Engineers historic daily tide data in coastal Louisiana. Louisiana Coastal Area, Science and Technology Office, 29 p.

Watson, C.S., N.J. White, J.A. Church, M.A. King, R.J. Burgette, and B. Legresy. 2015. Unabated global mean sea-level rise over the satellite altimeter era. Nature Climate Change, 5, 565-568.

Webb, E.L., D.A. Friess, K.W. Krauss, D.R. Cahoon, G.R. Guntenspergen, and J. Phelps. 2013. A global standard for monitoring coastal wetland vulnerability to accelerated sea-level rise. Nature Climate Change, 3, 458-465.

Woodroffe, C.D., R.J. Curtis, and R.F. McLean. 1983. Development of a chenier plain, Firth of Thames, New Zealand. Marine Geology, 53, 1-22.

Wöppelmann, G., C. Letetrel, A. Santamaria, M.-N. Bouin, X. Collilieux, Z. Altamimi, S.D.P. Williams, and B. Martin Miguez. 2009. Rates of sea-level change over the past century in a geocentric reference frame. Geophysical Research Letters, 36, L12607.

Wöppelmann, G. and M. Marcos. 2016. Vertical land motion as a key to understanding sea level change and variability. Reviews of Geophysics, 54, 64-92.

Xue, C. 1993. Historical changes in the Yellow River delta, China. Marine Geology, 113, 321-329.

Yi, S., Y. Saito, H. Oshima, Y. Zhou, and H. Wei. 2003. Holocene environmental history inferred from pollen assemblages in the Huanghe (Yellow River) delta, China: climatic change and human impact. Quaternary Science Reviews, 22, 609-628.

Zecchin, M., G. Brancolini, L. Tosi, F. Rizzetto, M. Caffau, and L. Baradello. 2009. Anatomy of the Holocene succession of the southern Venice lagoon revealed by very high-resolution seismic data. Continental Shelf Research, 29, 1343-1359.

FIGURES

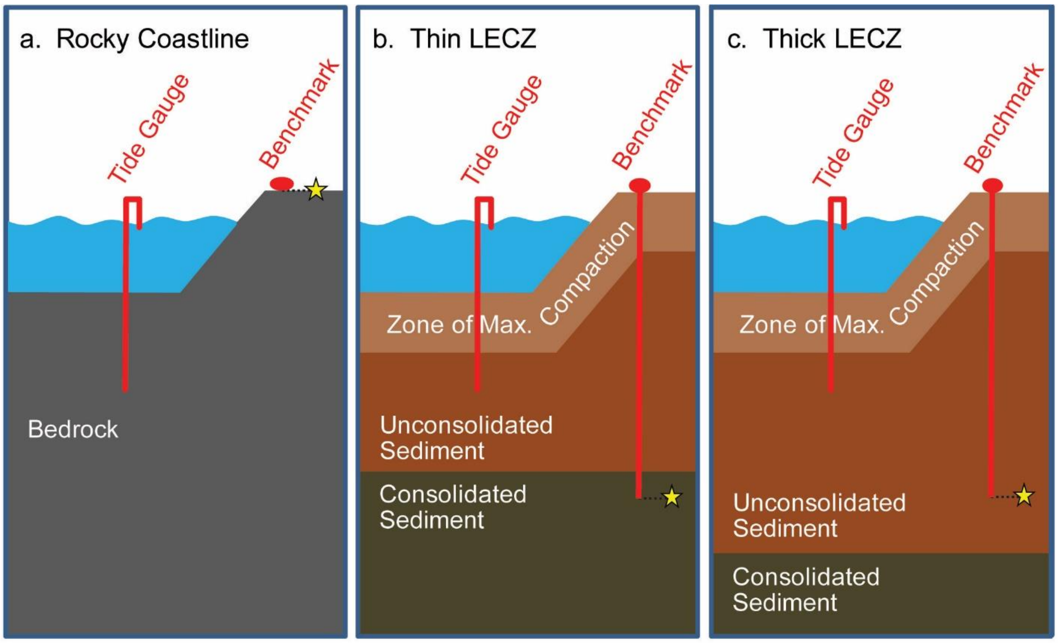

Figure 1: Schematic of a tide gauge and associated benchmark on a rocky coastline (a), a thin LECZ (b), and a thick LECZ (c). In all three environments, the tide gauge measures RSLR with respect to the base of the benchmark foundation, which is indicated by a star in each panel.

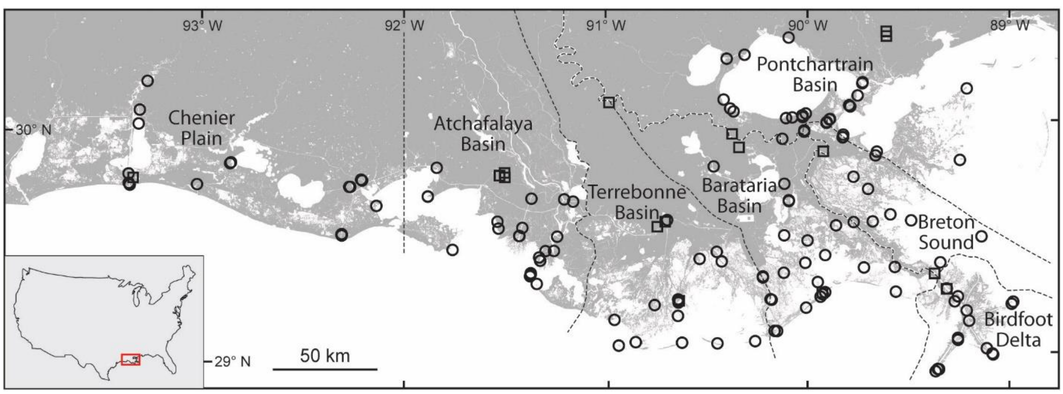

Figure 2: Location of tide gauges (circles, n = 131) and GPS stations (squares, n = 17) in the Holocene landscape of coastal Louisiana. Dashed lines delineate geographic areas discussed in the text.

Ocean Sci. Discuss., https://doi.org/10.5194/os-2018-75
Manuscript under review for journal Ocean Sci.
Discussion started: 23 July 2018

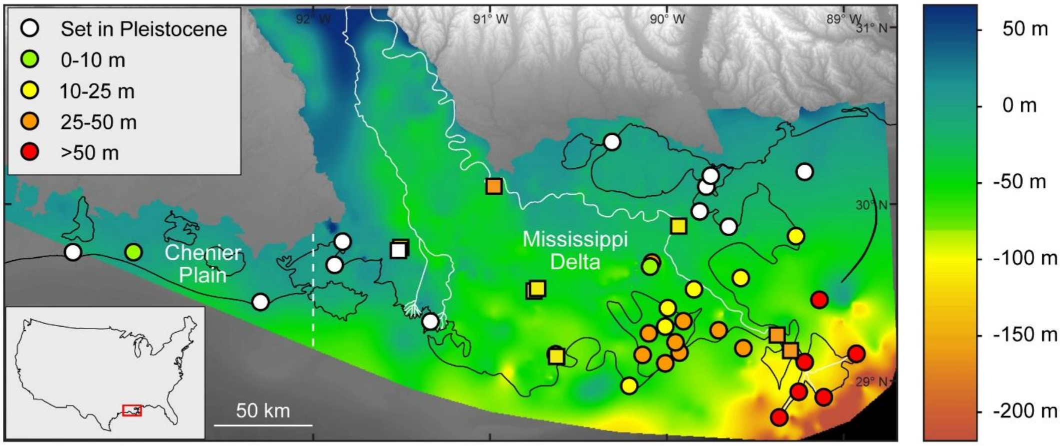

Figure 3: Elevation of the Pleistocene surface in coastal Louisiana (with respect to NAVD 88), which approximates the depth of the Pleistocene surface beneath the land surface given land surface elevations close to mean sea level. Circles and squares indicate tide gauge and GPS station locations, respectively, and are color coded according to foundation height above the Pleistocene surface. Note that two GPS stations (ENG1 and ENG2) have the same coordinates (and the same foundation depth) and plot on top of one another. The dashed white line, located at longitude 92° W, divides the Mississippi Delta from the Chenier Plain. Solid white lines show the Mississippi and Atchafalaya Rivers. Black lines indicate shorelines. Base map from Heinrich et al. (2015).

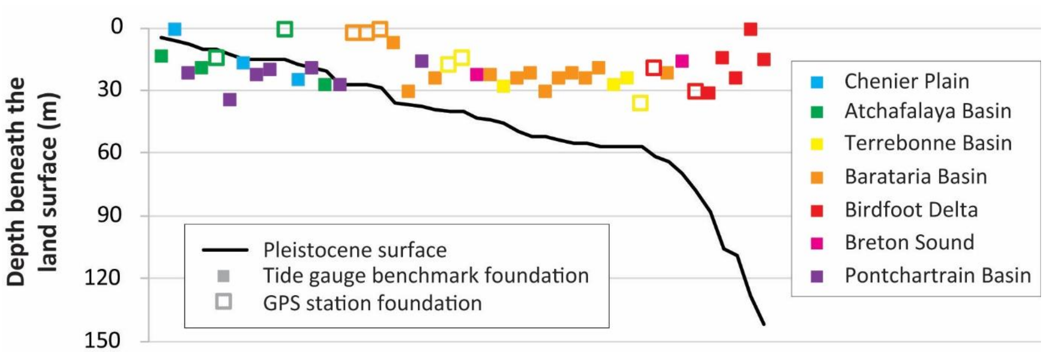

Figure 4: Schematic dip-oriented cross section comparing the depth of tide gauge benchmarks and GPS station foundations to the local depth to the Pleistocene surface. Sites are arranged by increasing depth of the Pleistocene surface. See Fig. 2 for the location of geographic areas.

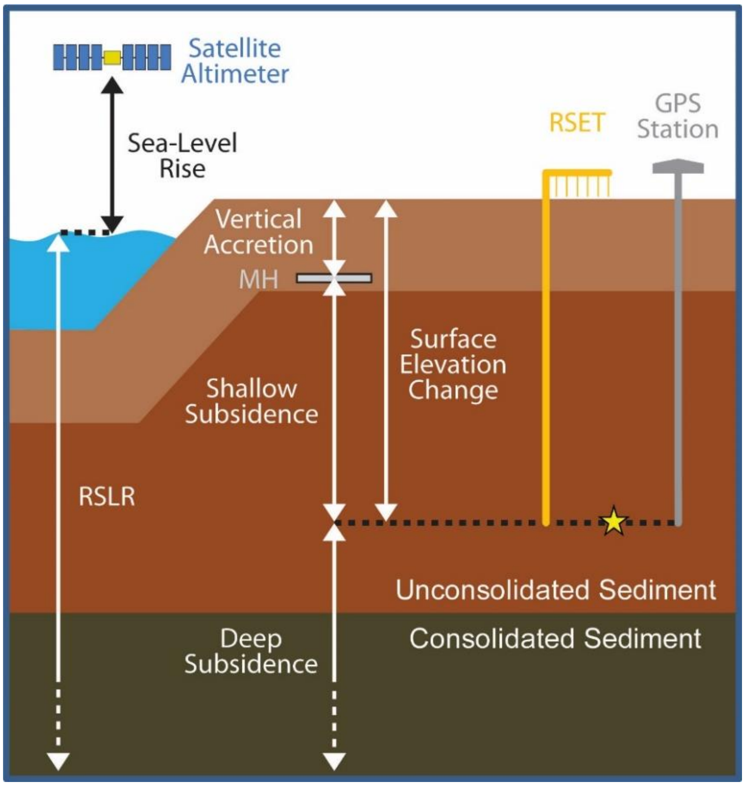

Figure 5. Schematic of combined instrumentation that includes a RSET-MH, which measures shallow subsidence, and a GPS station, which measures deep subsidence. To measure shallow subsidence using a RSET-MH, surface elevation change is subtracted from vertical accretion (Cahoon, 2015). Surface elevation change is the change in height from a horizontal arm at a fixed elevation to the wetland surface, measured using vertical pins. Vertical accretion is the thickness of material that accumulates above a feldspar marker horizon. If constructed with similar foundation depths (as shown by the star), the RSET-MH and GPS station collect data that are complementary and can be added together and combined with satellite altimetry data to calculate the rate of RSLR.

Ocean Sci. Discuss., https://doi.org/10.5194/os-2018-75
Manuscript under review for journal Ocean Sci.
Discussion started: 23 July 2018

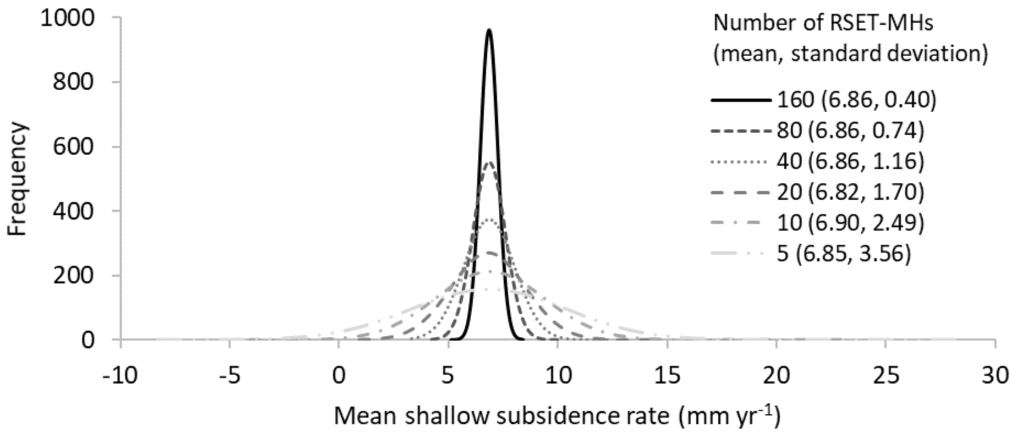

Figure 6. Probability density functions of the mean shallow subsidence rate for a given number of RSET-MHs, calculated using a Monte Carlo simulation and 10,000 randomizations per analysis. More detailed results for each of the six cases are presented in Fig. S1.

TABLES

Table 1: Tide gauges in the Holocene landscape of coastal Louisiana with known foundation information (*n* = 35).

Tide gauge name	Agency	Latitude	Longitude	Benchmark foundation depth (m)	Depth to Pleistocene surface (m)	Benchmark foundation height above Pleistocene surface (m)
Amerada Pass	NOAA	29.4500	-91.3383	27.4	21	Set in Pleistocene
Barataria Waterway	USACE	29.6694	-90.1106	7.4	36	29
Bay Gardene	NOAA	29.5983	-89.6183	23.2	43	20
Bay Rambo	NOAA	29.3617	-90.1400	24.4	54	30
Bayou Petit Caillou	USACE	29.2543	-90.6635	24.4	57	33
Bayou St. Denis	NOAA	29.4967	-90.0250	23.2	44	21
Billet Bay	NOAA	29.3717	-89.7517	21.9	52	30
Breton Island	NOAA	29.4933	-89.1733	16.8	70	53
Calcasieu Pass	NOAA	29.7683	-93.3433	25	18	Set in Pleistocene
Caminada Pass	NOAA	29.2100	-90.0400	21.9	55	33
Chef Menteur Pass	NOAA	30.0650	-89.8000	35.1	13	Set in Pleistocene
Comfort Island	NOAA	29.8233	-89.2700	16.8	38	21
Cypremort Point	NOAA	29.7133	-91.8800	19.4	10	Set in Pleistocene
East Bay	NOAA	29.0533	-89.3050	14.6	106	91
East Timbalier Island	NOAA	29.0767	-90.2850	28.8	46	17
Freshwater Canal Locks	NOAA	29.5517	-92.3050	17.1	15	Set in Pleistocene
Grand Isle	NOAA	29.2633	-89.9567	19.8	57	37
Grand Pass	NOAA	30.1267	-89.2217	23.2	15	Set in Pleistocene
Greens Ditch	NOAA	30.1117	-89.7600	21.9	8	Set in Pleistocene
Hackberry Bay	NOAA	29.4017	-90.0383	30.5	52	22
Lafitte	NOAA	29.6667	-90.1117	30.5	37	7
Lake Judge Perez	NOAA	29.5583	-89.8833	24.4	39	15
Leeville	NOAA	29.2483	-90.2117	28	57	29
Martello Castle	NOAA	29.9450	-89.8350	19.51	19	Set in Pleistocene
Mendicant Island	NOAA	29.3183	-89.9800	24.4	55	31
Mermentau River	USACE	29.7704	-93.0135	1.5	6	5
North Pass	NOAA	29.2050	-89.0367	15.2	142	127
Pass Manchac	NOAA	30.2967	-90.3117	20.7	15	Set in Pleistocene
Pelican Island	NOAA	29.2667	-89.5983	21.9	64	42
Pilottown	NOAA	29.1783	-89.2583	32	88	56
Port Eads	USACE	29.0147	-89.1658	0.9	128	127
Shell Beach	NOAA	29.8683	-89.6733	27.4	27	Set in Pleistocene
Southwest Pass	NOAA	28.9250	-89.4183	24.4	109	85
St. Mary's Point	NOAA	29.4317	-89.9383	24.4	50	26
Weeks Bay	NOAA	29.8367	-91.8367	14.3	5	Set in Pleistocene

Ocean Sci. Discuss., https://doi.org/10.5194/os-2018-75
Manuscript under review for journal Ocean Sci.
Discussion started: 23 July 2018

Ocean Science Discussions
Open Access

Table 2: GPS stations in the Holocene landscape of coastal Louisiana with known foundation information (*n* = 10).

GPS station code	Latitude	Longitude	Foundation depth (m)	Depth to Pleistocene surface (m)	Foundation height above Pleistocene surface (m)	Data source
AWES	30.10	-90.98	1	29	28	Karegar et al. (2015)
BVHS	29.34	-89.41	>20	62	<42	Dokka et al. (2006); Karegar et al. (2015)
ENG1	29.88	-89.94	~3	27	~24	Karegar et al. (2015)
ENG2	29.88	-89.94	~3	27	~24	Dokka et al. (2006)
FRAN	29.80	-91.53	14.7	10	Set in Pleistocene	Dokka et al. (2006)
FSHS	29.81	-91.50	1	15	14	Karegar et al. (2015)
HOMA	29.57	-90.76	18.3	40	22	Dokka et al. (2006)
HOUM	29.59	-90.72	>15	40	<25	Dokka et al. (2006); Karegar et al. (2015)
LMCN	29.25	-90.66	36.5	57	21	Dokka et al. (2006); Karegar et al. (2015)
VENI	29.28	-89.36	30.5	78	48	Dokka et al. (2006)

Table 3. Holocene sediment thicknesses of LECZs around the world, measured close to the shoreline where sediments tend to be the thickest.

Low-elevation coastal zone	Maximum thickness (m)	LECZ type	Reference
Chenier Plain, Miranda, New Zealand	3-5	thin	Woodroffe et al. (1983)
Chenier Plain, SW Louisiana, USA	5-10	thin	Heinrich et al. (2015)
Venice Lagoon, Italy	10-15	thin	Zecchin et al. (2009)
Chao Phraya Delta, Thailand	10-15	thin	Tanabe et al. (2003a)
Vistula Delta, Poland	10-20	thin	Mojski (1995)
Rhine-Meuse Delta, The Netherlands	20-25	thick	Hijma et al. (2009)
Huanghe Delta (modern), China	20-25	thick	Xue (1993); Yi et al. (2003)
Po Delta, Italy	20-25	thick	Amorosi et al. (2017)
Tokyo Lowland, Japan	20-60	thick	Tanabe et al. (2015)
Mekong Delta, Vietnam	25-40	thick	Ta et al. (2002); Tanabe et al. (2003b)
Nobi Plain, Japan	30-40	thick	Hori et al. (2011)
Shatt al-Arab Delta, Iraq	30-40	thick	Larsen (1975)
Nile Delta, Egypt	30-50	thick	Stanley and Warne (1993)
Song Hong Delta, Vietnam	35-40	thick	Funabiki et al. (2007)
Fly Delta, Papua New Guinea	35-45	thick	Harris et al. (1993)
Ganges-Brahmaputra Delta, Bangladesh	50-100	thick	Goodbred and Kuehl (2000)
Mississippi Delta, SE Louisiana, USA	50-100	thick	Heinrich et al. (2015)
Yangtze Delta, China	60-90	thick	Li et al. (2000)
Indus Delta, Pakistan	110-120	thick	Clift et al. (2010)